Biophysical Chemistry, 46 (1993) 237–248
Elsevier Science Publishers B.V., Amsterdam

BIOCHE 01742

Tryptophan mutants of human C5a anaphylatoxin: A fluorescence anisotropy decay and energy transfer study

M. Federwisch [a], A. Wollmer [a,*], M. Emde [b], T. Stühmer [b], T. Melcher [b], A. Klos [b], J. Köhl [b] and W. Bautsch [b]

[a] *Institut für Biochemie, Rheinisch-Westfälische Technische Hochschule Aachen, Klinikum, Pauwelsstr. 30, D-5100 Aachen (Germany)*
[b] *Institut für Medizinische Mikrobiologie, Medizinische Hochschule Hannover, Konstanty-Gutschow-Straße 8, D-3000 Hannover 61 (Germany)*

(Received 30 September 1992; accepted in revised form 16 November 1992)

Abstract

Three mutants of the anaphylatoxin C5a were prepared with positions 2, 64 and 70, respectively, substituted by tryptophan. The last mutant was additionally labelled at Cys^{27} for fluorescence energy transfer (FET) measurements. The structural integrity and biological activity of the molecules were not affected. Fluorescence anisotropy decay (FAD) measurements showed that the rotational correlation time for tryptophan decreases in the order: [Trp^2]rhC5a > [Trp^{64}]rhC5a > [Trp^{70}]rhC5a, indicating an increasing mobility of the side chain. Measurements of the fluorescence energy transfer from Trp^{70} to the 1,5-AEDANS group at Cys^{27} yielded a distance distribution of 2.4 ± 0.8 nm. This value is compatible with the C-terminal chain being arranged as a slightly stretched helix pointing away from the body of the molecule.

Keywords: Complement peptide C5a; C5a mutants (biosynthetic analogues); Fluorescence energy transfer; Time-resolved fluorescence; Comparison with NMR structure

1. Introduction

Among the anaphylatoxins, the 74 amino acid C5a protein derived from the complement system is one of the principal inflammatory molecules because of its broad range of biological properties [1,2]. Compared to the number of studies of the biological function of C5a, relatively few experiments have been carried out to investigate its structure. The tertiary structure of bovine [3], recombinant human [4], and porcine [5] C5a in solution were determined from nuclear magnetic resonance data (NMR). Interpretation of the NMR data of recombinant human C5a (designated rhC5a) suggests chain segments 4–12, 18–26, 34–39, and 46–63 to be helical. The C-terminal helix looses stability beyond residue 63 and gradually becomes ill-defined [4]. However, it is the very C-terminus of the molecule beyond Ala^{63} that contains residues essential for receptor interaction as shown with rhC5a mutants [6] and represents the effector site of the molecule as shown by C5a peptide analogues [7,8]. These studies showed that Lys^{68}, Leu^{72} and the C-terminal Arg^{74} are involved in receptor interaction; in addition, substitution of fully aromatic side chains for His^{67}

* To whom correspondence should be addressed. Telephone: (0241) 808 8850, Telefax: (0241) 808 8851.

markedly increased activity. Still other ligand–receptor interactions, however, are required for full expression of potency [8]. In contrast, the N-terminal dodecapeptide probably simply serves to stabilize the C5a conformation [6].

The related 77 amino acid human C3a (hC3a) and hC5a anaphylatoxins have 36% sequence identity, and both the disulfide and helix patterns of the two proteins are largely the same [4]. The C-terminal residues 67–70 of hC3a (corresponding to residues 64–67 of hC5a) may transiently adopt helical conformation [9]. In the crystal structure of hC3a the C-terminal helix even extends to residue 73 [10]. A model of hC5a was presented, based on comparative methods, in which the C-terminal helix also extends till residue 73 [11].

To gain further experimental insight into the solution structure of human C5a, especially of the functionally important C-terminus, we prepared three mutants with a Trp residue in position 2, 64 and 70, respectively, which were expected and confirmed to be fully active. The structural integrity of the mutants was confirmed by circular dichroism (CD) spectroscopy. Tryptophan mutants are particularly attractive since native C5a contains no Trp and only one Phe and two Tyr residues. Their fluorescence spectra and intensity decays predominantly reflect the local Trp environment [12,13] and fluorescence anisotropy decays (FAD) provide independent information on Trp side-chain dynamics.

Since the tyrosyl fluorescence intensity of rhC5a was too low for measuring the energy transfer (FET) to the Trp residue, [Trp^{70}]rhC5a was additionally labelled by *N*-iodoacetyl-*N'*-(5-sulfo-1-naphthyl)ethylenediamine (1,5-I-AEDANS) at Cys^{27}, which is pointing into the solution [4]. This derivative is designated [Trp^{70}]rhC5aD.

2. Materials and methods

2.1. Preparation of the mutants

The spectroscopic studies were carried out with recombinant human C5a (rhC5a) and rhC5a mutants. Cloning, purification and characterization of rhC5a was described elsewhere [2]. Structurally, rhC5a is identical with human serum C5a except for the presence of a β-mercaptoethanol molecule disulfide bonded to Cys^{27} and the absence of the carbohydrate chain at Asn^{64}; in addition, about 20% of the molecules contain an additional N-terminal methionine which does not interfere with biological activity. Tryptophan mutants at position 2, 64, and 70 of the native hC5a sequence were prepared by PCR-mediated site-directed mutagenesis of plasmid pME10 containing the hC5a coding DNA sequence [2]. Oligonucleotides: P1 (5'-ACGCTGCAAAAGAAGATAGAA-3'), P2 (5'-GCTGCAGCTATTATTACCTTCCCAATTGCA-3'), P3 (5'-ACGTGGCAAAAGAAGATAGAA-3'), P4 (5'-GCGCGCTTGGATCTCTCATAAAGACA-3'), P5 (5'-CCAAGCGCGCAGCTGGCT-3') and P6 (5'-GCTGCAGCTATTATTACCTTCCCAATTGCCAGTCT-3') were synthesized on a Gene Assembler Plus (Pharmacia LKB Biotechnology, Piscataway, NJ, USA) and purified by gel chromatography on NAP-10 columns (Pharmacia) in distilled water. PCR-mediated mutagenesis of pME10 was performed as described in detail elsewhere [14] using P2/P3 as amplification primers for obtaining the [Trp^{2}]rhC5a mutant, and P1/P6 for obtaining the [Trp^{70}]rhC5a mutant. For preparation of the [Trp^{64}]rhC5a mutant a two-step amplification scheme was employed as described in detail elsewhere [15]: Two partial DNA fragments for [Trp^{64}]rhC5a were prepared by separate PCR amplification reactions of pME10 with the primer pairs P2/P4 and P1/P5, respectively. Subsequently, 1 μl aliquots of both reactions were combined and the full [Trp^{64}]rhC5a sequence obtained by amplification with P1/P2. The PCR fragments were subcloned into plasmid pKK233-2 (Pharmacia) and completely sequenced to confirm the correct sequence. The proteins were expressed in *E. coli* and purified to homogeneity as described previously for rhC5a [2].

The amino acid composition of all mutants was determined by quantitative amino acid analysis on a Biotronik LC 5001. Briefly, the hydrolysate of a protein or peptide is separated by ion ex-

change chromatography [16]. Postcolumn derivatization with *o*-phthaldialdehyde (OPT) [17] serves to detect the amino acids by fluorescence.

The biological activity of the mutants was quantified by the myeloperoxidase release assay from human granulocytes [18].

2.2. Labelling

Since human C5a contains a free cysteine (Cys^{27}) [Trp^{70}]rhC5a was labelled with *N*-iodoacetyl-*N'*-(5-sulfo-1-naphthyl)ethylene-diamine (1,5-I-AEDANS, Sigma). The thiol reactive label, described by Hudson and Weber [19], was introduced according to the producedure of Wang and Cheung [20]. Briefly, to remove the β-mercaptoethanol from Cys^{27} without affecting the cystines [Trp^{70}]rhC5a was incubated for 60 minutes by 1,4-dithiothreitol (DTT) (molar ratio 2:1) at room temperature [21]. Then a 1.5-fold molar excess of 1,5-I-AEDANS was added to [Trp^{70}]rhC5a and the sample left in the dark at room temperature for 24 h. Unreacted label was removed by dialysis. For every step degased 50 m*M* potassium phosphate buffer, pH 7.6, containing 1 m*M* EDTA was used. Since the degree of labelling is usually non-stoichiometric, the fractional occupancy of the acceptor site, f_A, was calculated by dividing the concentration determined at 337 nm (AEDANS absorption) by the protein concentration determined by quantitative amino acid analysis.

N-Acetyl-L-tyrosinamide was supplied by Sigma. All other chemicals are commercially available and were of p.a. grade. The water was prepared with a Milli-Q system (Millipore S.A., Mulhouse, France).

2.3. Solutions

The mutants were dissolved in 50 m*M* potassium phosphate standard buffer, pH 7.5. Concentrations were determined photometrically using a Pye-Unicam PU 8800 UV/VIS spectrophotometer (Philips, Kassel, Germany). The molar extinction coefficients used here are $\epsilon_{277} = 4{,}595\ M^{-1}\ cm^{-1}$ for rhC5a, $\epsilon_{278} = 11{,}300\ M^{-1}cm^{-1}$ for [Trp^2]rhC5a and [Trp^{70}]rhC5a (based on quantitative amino acid analysis), and $\epsilon_{337} = 6{,}000\ M^{-1}\ cm^{-1}$ for [Trp^{70}[rhC5aD [19]. Calculation of the extinction coefficient from the number of aromatic amino acids and cystines [22] yields lower values. The reason for this discrepancy (the theoretical values were about 20% lower) remains unclear. Hugli and Müller-Eberhard determined $\epsilon_{276} = 11{,}100\ M^{-1}cm^{-1}$ for native human C5a and $\epsilon_{276} = 3280\ M^{-1}cm^{-1}$ for rat C5a [23] (hence, owing a greater discrepancy). For fluorescence measurements the concentrations were adjusted to an optical density ≤ 0.1 (1 cm) at the wavelength of their excitation. All measurements were carried out at 22°C.

2.4. Spectroscopy

CD measurements were carried out on an AVIV (Lakewood, NJ, USA) 62 DS CD spectrometer calibrated with a 0.1% aqueous solution of d-10-camphorsulphonic acid [24]. Further details were described earlier [25]. To determine the secondary structural composition the spectra were analysed with the CONTIN [26] and VARSELEC [27] program package.

The steady-state fluorescence spectra were recorded on a Spex Fluorolog 211 photon counting spectrofluorimeter (Spex Industries, NY, USA.) with a bandwidth of 2.7 nm (excitation monochromator) and 2.2 nm (emission monochromator). They are corrected for changes in the lamp intensity and for spectral sensitivity of the emission monochromator-photomultiplier system.

2.5. Time-resolved fluorescence

Fluorescence intensity and fluorescence anisotropy decays (FAD) were measured in the single photon counting mode with an Edinburgh Instruments Ltd. (UK) spectrometer, Model 199.

The excitation wavelengths were 275 nm for Tyr, 275, 295 and 300 nm for Trp, and 340 nm for AEDANS. Depending on the intensity the bandwidth varied from 8 to 14 nm. The emission was passed through a combination of a UV transmitting black glass and cut-off glass filter to create a bandpass (WG 305 and DUG 11 in the case of Tyr and WG 335 and UG 11 in the case of Trp)

or a cut-off filter (KV 389 in the case of AEDANS). All filters were supplied by Schott (Mainz, Germany). Cumulation was stopped when at least 80,000 counts were stored in the peak channel for the total fluorescence intensity decay, $S(t)$.

The "g-factor" of the system which is necessary to calculate the anisotropy $R(t)$ was determined using either a solution of hexameric insulin or 1-cyanonaphthalene in ethanol. Both of them were excited at 290 nm with the polarizer turned horizontal. The resulting decays I_{hv} and I_{hh} with the analyzer in vertical and horizontal position, respectively, were integrated to calculate $g = \langle I_{hv} \rangle / \langle I_{hh} \rangle$, yielding $g = 1$.

The lamp pulse $L(t)$ of the thyratron-gated hydrogen flashlamp was recorded with a Ludox (Du Pont, Wilmington, DE, USA) suspension using incident light at the wavelength of maximum fluorescence of the fluorophores. It has a full width at half maximum (FWHM) of ~ 1.4 ns.

Since the deconvolution technique used is limited only by the stability of the instrument and the light source, fluorescence lifetimes as short as 0.2 ns can be determined with this instrument despite the broader FWHM [28]. Using synchrotron radiation and a conventional photomultiplier tube for detection Munro et al. [29] calculated that rotational correlation times, ϕ, as short as 0.1 ns can be measured. The flashlamp employed here may have a slightly reduced stability compared to the synchrotron radiation but the time-jitter resulting from the photomultiplier is the same, hence, a lower limit of 0.2 ns for the determination of ϕ seems reasonable.

Data handling and the iterative non-linear least-squares fit of the decays were accomplished by a program supplied by Edinburgh Instruments Ltd. The quality of fit was judged by the reduced Chi-squared, χ^2. The weighted residuals were checked for random distribution [30]. The analyses of the FAD measurements were as described previously [31].

2.6. Fluorescence energy transfer (FET)

According to Förster's theory the fluorescence energy is transferred with efficiency E from the donor to the acceptor which is dependent of the distance, r, between the centres of the donor and acceptor chromophores and the so-called Förster distance, R_0, at which E is 50%. According to Stryer [32]:

$$E = R_0^6 / (R_0^6 + r^6) \tag{1}$$

$$R_0^6 = \left(J k^2 Q_D n^{-4}\right)^{1/6} \times 9.7 \times 10^3 \text{ Å} \tag{2}$$

The variables of R_0^6 are: J, the spectral overlap integral; k^2, the orientation factor for a dipole–dipole interaction; Q_D the quantum yield of fluorescence of the energy donor in the absence of the acceptor; n, the refractive index of the medium between the donor and the acceptor ($n = 1.36$, water).

The spectral overlap integral J (in $cm^3 M^{-1}$) is defined as:

$$J = \frac{\int F_D(\lambda) \epsilon_A(\lambda) \lambda^4 \, d\lambda}{\int F_A(\lambda) \, d\lambda} \tag{3}$$

where $F_D(\lambda)$ is the fluorescence intensity (in arbitrary units, a.u.) of the energy donor at the wavelength λ (in cm), and $\epsilon_A(\lambda)$ is the extinction coefficient (in $cm^{-1} M^{-1}$) of the energy acceptor. J was numerically integrated at 1 nm steps.

The major error in measuring distances by FET is due to uncertainties in the orientation factor, k^2. This is often assumed to be equal to 2/3, which is strictly justified only if the two transition dipoles undergo a random dynamic reorientation which is rapid in comparison with the decay of the excited state [33]. Dale et al. [33] delineate upper and lower bound from FAD measurements and, hence, the maximum uncertainity in the distance due to the unknown value of k^2. But in practice the transitions are often mixed. In this case, the calculations of Haas et al. [34] sets limits to k^2 which are much closer to the value of random orientation, 2/3. As compared to the influence of k^2, the effect of the errors in Q_D and J, as well as of the uncertainty in n, were considered to be negligible [35].

Fluorescence quantum yields, Q, were determined by the comparative method [36] using quinine sulfate in 1 N sulphuric acid as a fluores-

cence standard, $Q_{St} = 0.55$ for $c = 10^{-5}$ M at 22°C, excitation at 365 nm [37].

The transfer efficiency can be determined from the relative fluorescence yield of the donor F_D in the absence and F_{DA} in the presence of the acceptor or the lifetimes of the donor under the respective conditions (τ_D and τ_{DA}). The fractional occupancy of the acceptor site, f_A, was introduced into the calculation of E [20]:

$$E = 1 - \frac{F_{DA} - F_D(1 - f_A)}{F_D f_A}$$

or

$$E = 1 - \frac{\tau_{DA} - \tau_D(1 - f_A)}{\tau_D f_A} \quad (4)$$

These two measurements will yield identical results only when the separation between donor and acceptor is a well defined and constant quantity [38]. Furthermore, if the total fluorescence intensity decay of the donor is not mono-exponential (as it mostly is with Trp) it has to be assumed that only a single and constant value of R_0 is associated with all of the decay modes [39]. This is reasonable since the intensity decays of proteins are only weakly dependent of the emission wavelength [40]. Then an average decay time, $\langle\tau\rangle$, can be calculated:

$$\langle\tau\rangle = \sum B_i\tau_i = \sum \left[\frac{b_i\tau_i}{\sum b_j\tau_j} \right] \tau_i; \quad i, j = 1, 2, \cdots, n \quad (5)$$

(b_i and τ_i are the amplitude and lifetime of the ith decay mode, respectively) and used instead. Furthermore, it is possible to determine the average distance and the width of the distance distribution by combined measurement of fluorescence intensity and average decay time [39], if the separation is not constant.

3. Results and discussion

3.1. Preparation and characterization of the mutants

Tryptophan residues were introduced into rhC5a one by one at three different positions which were expected or had previously been shown not to interfere with biological activity and/or structure to ensure that all structural information obtained with these mutants would also be relevant for native rhC5a. A good candidate for such a Trp substitution was Asn^{64} as this amino acid carries an oligosaccharide moiety in native hC5a which had previously been shown to have no influence on the biological activity [41]. In addition, this is the first position of the C5a C-terminus for which no definite structural information was obtainable by NMR spectroscopy. Being fairly close to the very C-terminus of the molecule, Met^{70} had already safely been mutated into a tryptophan residue before [6]. And finally, Leu^2 was exchanged for a Trp to check independently whether (in contrast to hC3a) the N-terminal residues in hC5a are attached to the core. This residue had also been excluded previously as a receptor-interacting residue [6].

All mutants were expressed and purified to homogeneity from *E. coli* and showed full C5a activity in the myeloperoxidase release assay from human granulocytes (Table 1). [Trp^{70}]rhC5a exhibited a slightly increased (though insignificant with respect to receptor interaction) activity (about two-fold) in good agreement with previous observations [6].

To allow for intramolecular FET measurements, the [Trp^{70}]rhC5a mutant was labelled by the thiol-reacting 1,5-I-AEDANS group to yield [Trp^{70}]rhC5aD. This compound displayed the same biological activity as [Trp^{70}]rhC5a (Table 1). Since its CD spectrum was identical to rhC5a, too (see below), we conclude that only Cys^{27} has been labelled as it is well known from previous studies

Table 1

Biological activity (ED_{50} values in nM; mean ± s.d.) of rhC5a and tryptophan mutants in the myeloperoxidase release assay from human granulocytes. (n = no. experiments)

Mutant	ED_{50} [nM]	C5a activity [%]
rhC5a	0.97 ± 0.19	100 (n = 8)
[Trp^2]rhC5a	0.84 ± 0.17	115 (n = 2)
[Trp^{64}]rhC5a	0.78 ± 0.16	124 (n = 2)
[Trp^{70}]rhC5a	0.47 ± 0.04	206 (n = 2)
[Trp^{70}]rhC5aD	0.49 ± 0.08	198 (n = 2)

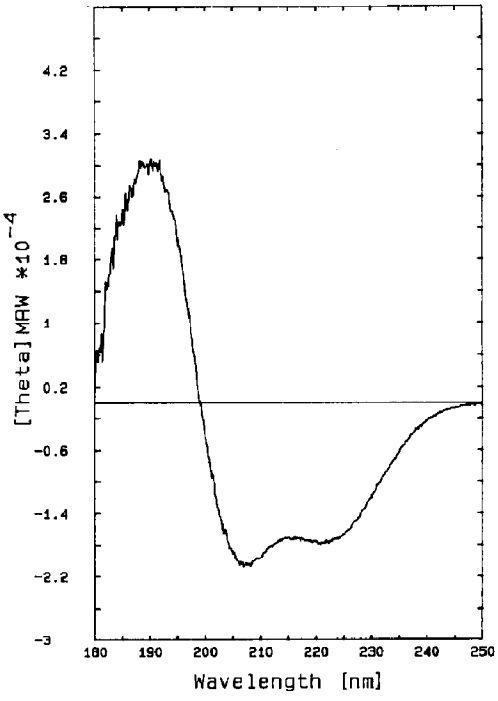

Fig. 1. Far UV CD spectrum of rhC5a.

that the integrity of the secondary conformation of the C5a molecule is largely dependent on disulfide bonds and essential for its full activity [42].

3.2. CD measurements

Figure 1 shows the far-UV CD spectrum of rhC5a. The results of the secondary structural analyses are given in Table 2. They are in good agreement with earlier results: The α-helix content of bovine and porcine C5a were determined by CD spectroscopic analysis to be about 42% [43] and 40% [23].

The NMR data mainly reveal helices and turns. A conservative interpretation locates helices in

Table 2

Secondary structural analysis results of rhC5

Program package	Helix	β-Sheet	β-Turn	Remainder
CONTIN [26]	41.7%	21.1%	25.3%	12%
VARSELEC [27]	42 %	12 %	27 %	16 %

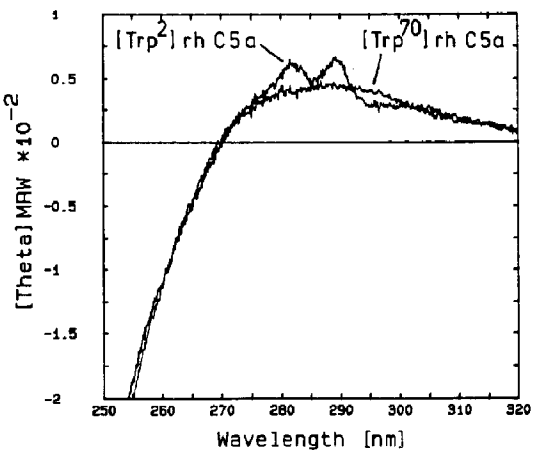

Fig. 2. Near UV CD spectrum of [Trp^2]rhC5a and of [Trp^{70}]rhC5a.

the chain segments 4–12, 18–26, 34–39, and 46–63 [4], which are making up for $42 \times 100/74 = 57\%$ of the residues of hC5a.

The far-UV CD spectra of all mutants were identical in shape and are therefore not shown. The absolute ellipticity varied slightly, which is probably due to remaining uncertainties in protein concentration. Hence, all mutants including the labelled one are structurally the same as native C5a.

The near-UV spectrum of [Trp^2]rhC5a exhibits a fine structure typical of a restricted Trp side-chain motion (Fig. 2).

3.3. Steady-state fluorescence

Figure 3 shows the fluorescence spectra of rhC5a, [Trp^2]rhC5a, [Trp^{70}]rhC5a, and [Trp^{70}]-rhC5aD. The spectrum of [Trp^{64}]rhC5a was omitted for the sake of simplicity because it was similar to [Trp^{70}]rhC5a apart from a slightly lower intensity. The spectra are corrected for differences in the optical density at the excitation wavelength. The Trp mutants were excited at 295 nm, native rhC5a at 275 nm.

The fluorescence intensity of rhC5a is very low. Compared to *N*-acetyl-L-tyrosinamide dissolved in 25 m*M* Tris buffer the relative quantum yield Q_{rel}, of *N*-acetyl-L-tyrosinamide dissolved in 50 m*M* phosphate buffer, pH 7.8, is 0.85, due to the interaction with the phosphate ion [44]. But Q_{rel} of rhC5a is only 0.08. This

implies that the fluorescence of both Tyr residues is quenched and the influence of the buffer can be neglected. According to Cowgill (Table 2 in [45]) such a strong quenching can originate only in a disulfide group within van der Waals distance of the aromatic ring. This is trivial in the case of Tyr^{23} which is adjacent to Cys^{22}. According to Mollison et al. (Fig. 2 in [6]) Tyr^{13} is likely to interact with cystine (21–47).

The Trp fluorescence of [Trp^2]rhC5a excited at 295 nm has its λ_{max} at 338 nm and a full width at half maximum (FWHM) of 55 nm, while in the case of [Trp^{64}]rhC5a and [Trp^{70}]rhC5a λ_{max} is 349 and FWHM 63 nm (see Fig. 3). Hence, Trp^2

Table 3

Fluorescence lifetime (A) and anisotropy decay data (B) of the mutants. λ_{exc} is the excitation wavelength, B_i and τ_i are the amplitude and lifetime of the ith excited state, respectively, χ^2 the reduced Chi-squared, $\langle\tau\rangle$ the average decay time (5), r_i the fitted anisotropies, ϕ_i the corresponding rotational correlation times. The limiting anisotropies are: $r(t \rightarrow 0) = r_0 = r_1 + r_2 + r_\infty$, $r(t \rightarrow \infty) = r_\infty$. P10 and P11 are based on the C-terminus of human C3a, bold one-letter symbols of amino acid residues correspond to its native sequence. P10: **LRRQAWRASALGLAR**, P11: **CNYITELRQRHARASHLGLAR**

(A) Fluorescence lifetime

Mutant	λ_{exc} (nm)	B_1	B_2	B_3	τ_1 (ns)	τ_2 (ns)	τ_3 (ns)	χ^2	$\langle\tau\rangle$ (ns)
rhC5a	275	0.53	0.29	0.18	0.21	2.52	7.97	1.10	2.28
[Trp^2]rhC5a	275	0.09	0.43	0.48	0.94	3.21	6.16	1.12	4.42
[Trp^2]rhC5a	300	0.10	0.38	0.52	1.13	3.46	6.26	1.05	4.68
[Trp^{64}]rhC5a	295	0.17	0.64	0.19	0.48	2.88	5.22	1.12	2.92
[Trp^{70}]rhC5a	275	0.17	0.60	0.23	0.86	2.90	5.84	1.13	3.23
[Trp^{70}]rhC5a	295	0.17	0.60	0.23	0.73	2.88	5.94	1.10	3.22
[Trp^{70}]rhC5a	300	0.19	0.59	0.22	0.98	2.97	5.91	1.10	3.24
[Trp^{70}]rhC5aD	295	0.25	0.53	0.22	0.62	2.48	5.50	1.31	2.68
[Trp^{70}]rhC5aD	340	0.02	0.15	0.83	0.60	9.11	16.98	1.26	15.47
P10	290	0.28	0.65	0.07	0.86	2.75	9.45	1.47	2.69
P11	274	0.47	0.45	0.08	0.68	1.74	8.12	1.30	1.75

(B) Anisotropy decay

Mutant	λ_{exc} (nm)	r_0	r_1	r_2	r_∞	ϕ_1 (ns)	ϕ_2 (ns)	χ^2
rhC5a	275	0.168	0.132	–	0.036	0.26	–	1.12
[Trp^2]rhC5a	275	0.147	0.130	–	0.017	6.05	–	0.99
[Trp^2]rhC5a	300	0.226	0.206	–	0.020	5.85	–	1.05
[Trp^{64}]rhC5a	295	0.083	0.079	–	0.004	3.47	–	1.17
[Trp^{70}]rhC5a	275	0.107	0.081	–	0.026	1.80	–	1.16
[Trp^{70}]rhC5a	275	0.228	0.145	0.061	0.022	≤ 0.20 [a]	2.53	1.04
[Trp^{70}]rhC5a	295	0.107	0.080	–	0.027	1.65	–	1.04
[Trp^{70}]rhC5a	295	0.127	0.056	0.049	0.022	0.43	3.11	0.96
[Trp^{70}]rhC5a	300	0.154	0.120	–	0.034	1.68	–	1.37
[Trp^{70}]rhC5a	300	0.180	0.081	0.074	0.025	0.51	3.44	1.13
[Trp^{70}]rhC5aD	295	0.094	0.075	–	0.019	1.59	–	1.14
[Trp^{70}]rhC5aD	295	0.117	0.055	0.048	0.014	0.32	3.02	1.06
[Trp^{70}]rhC5aD	340	0.171	0.160	–	0.011	5.17	–	1.27
P10	290	0.097	0.090	–	0.007	0.54	–	1.15
P11	274	0.120	0.112	–	0.008	0.58	–	1.55

[a] See Materials and methods.

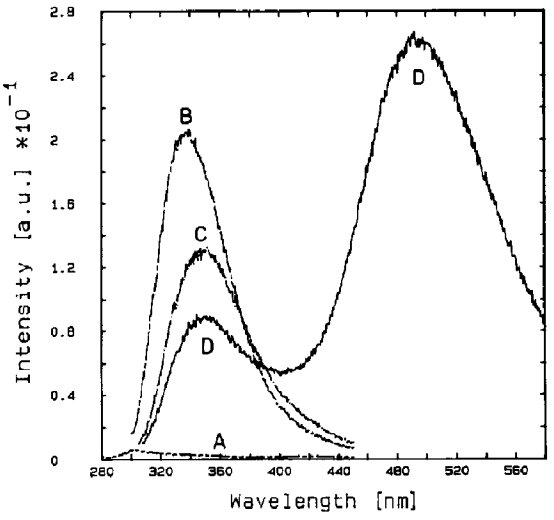

Fig. 3. Fluorescence spectra of (A): rhC5a, excitation wavelength 275 nm, and (B): [Trp^2]rhC5a, (C): [Trp^{70}]rhC5a, and (D): [Trp^{70}]rhC5aD, excitation wavelength 295 nm. The intensities are corrected for differences in the optical density at the excitation wavelength.

belongs to class II Trp residues, being immobilized though in limited contact with water, while Trp^{64} and Trp^{70} belong to class III residues, being completely exposed to water [46].

3.4. Time-resolved fluorescence

The results of the time-resolved measurements are given in Table 3. All decays of the total fluorescence intensity appear to be best described by triple exponentials. This is in accordance with the literature where multiple lifetimes are reported for proteins containing a single Trp or Tyr residue [47].

Comparison of the average decay time of rhC5a and P11, which both show Tyr fluorescence, reveals that the decay of rhC5a is not affected by the strong quenching observed in the steady state. Hence, the quenching is mainly static in the case of rhC5a. P10 and P11 are peptides whose sequence is nearly identical with the C-terminus of hC3a. Their data are included for comparison because they contain a single Trp or Tyr and are known not to adopt a regular conformation [31].

The average decay time, $\langle\tau\rangle$, of the Trp mutants increases with decreasing exposure to the aqueous environment, hence, they are not quenched within the protein matrix. The lowest value of $\langle\tau\rangle$ is obtained with P10. Figure 4A shows the decay of the total fluorescence intensity of [Trp^{70}]rhC5a.

The 1,5-AEDANS group within [Trp^{70}]rhC5aD possesses an average decay time of 15.5 ns and a λ_{max} of 496 nm. Both values are indicating that the polarity in its environment is equal to 60% ethanol in an ethanol–water mixture [19]. Hence, the label does not tumble freely in solution but probably is attached to a hydrophobic patch on the surface of [Trp^{70}]rhC5aD.

Fitting the anisotropy decay of the Tyr residues results in a very short rotational correlation time, ϕ, of 0.26 ns which is close to that of free tyrosine ($\phi = 0.1$ ns, [48]) indicative of nearly unrestricted side-chain movement. Nevertheless, neither of them escapes static quenching by the cystine as is obvious from the very low Q_{rel} (see above). While Tyr^{23} is involved in hydrophobic interactions between the N-terminal helix and the core and partially exposed Tyr^{13} is buried in a hydrophobic cavity [4]. This must not necessarily freeze side-chain mobility [29]. In tetrameric melittin, for instance, the Trp side-chains are located in a relatively wide hydrophobic pocket. The shortest correlation time which had to be fitted was 0.06 ns [49].

The rotational correlation times of the Trp's and AEDANS, resulting from a mono-exponential fit, can be divided into three classes: $\phi \sim 5.5$ ns, ~ 3.5 ns and ~ 1.5 ns. It is tempting to attribute the longest ϕ to the overall rotation. The decreasing ϕ indicates that the mobility increases from Trp^2 and AEDANS-Cys^{27} to Trp^{64} and Trp^{70}. For [Trp^{70}]rhC5a the anisotropy decay had to be fitted with two correlation times. Careful inspection of the residuals (Fig. 4B) shows that otherwise a nonrandom damped oscillation is superimposed. The results are: $\phi_1 \sim 0.4$ ns and $\phi_2 \sim 3.0$ ns (Table 3B), with the shorter ϕ attributable to the side-chain mobility and the longer to the overall rotation. Since the two are not completely independent, the second one is reduced.

The error associated with the rotational correlation times can be estimated from a comparison

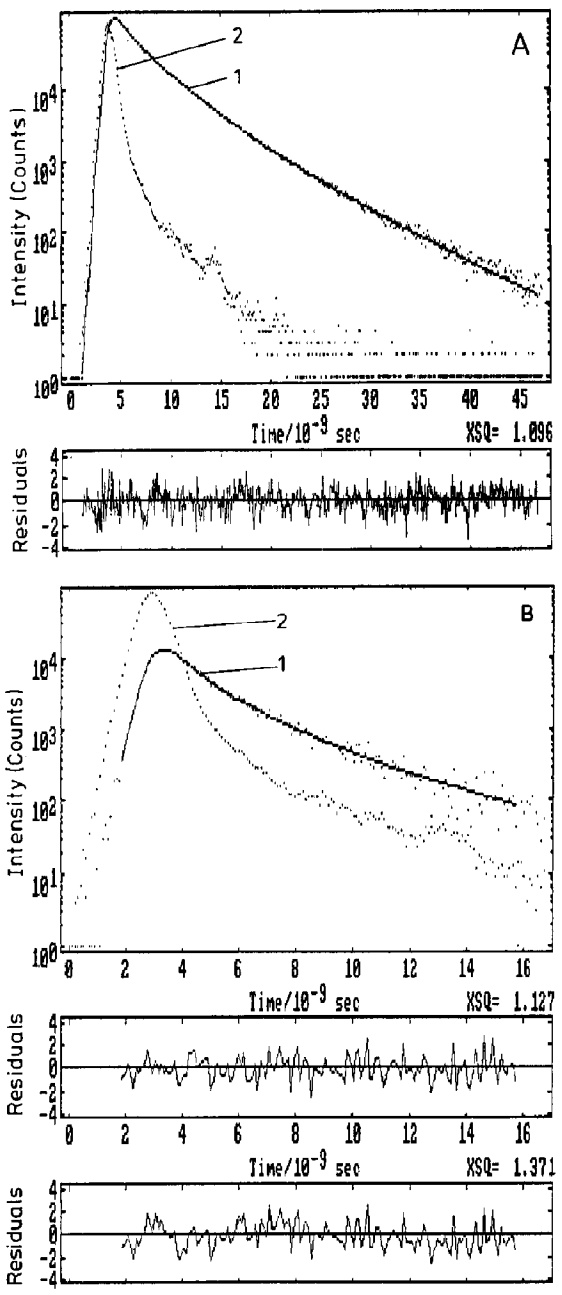

Fig. 4. Time-resolved fluorescence of the [Trp[70]]rhC5a. (A) The decay of the total fluorescence intensity $S(t)$ fitted with three lifetimes. (B) The decay of the difference $D(t)$ between the intensities of polarized fluorescence fitted with a single rotational correlation time ($\chi^2 = 1.371$) and below the residuals of the fit with two rotational correlation times ($\chi^2 = 1.127$). Dots: (1) measured decay: excitation wavelength: 300 nm; bandwidth: 14 nm; filter: WG 335, UG11. (2) lamp pulse measured at 340 nm. Continuous line: fitted decay. The parameters are given in Table 3.

of the values given in Table 3B. The anisotropy decay for Trp[2] was measured two times, and that for Trp[70] four times. (It does not matter that the excitation wavelengths were different.) The two correlation times obtained for Trp[2] (5.85 and 6.05 ns) differ by 0.2 ns. The four values for Trp[70] obtained by fitting a single correlation time vary within the limits 1.59 and 1.80 ns, i.e. an interval of 0.21 ns. Fitting two correlation times implies more adjustable parameters and, hence, broader variation. The four values of ϕ_1 vary within the limits of ≤ 0.2 and 0.51 ns, those of ϕ_2 within 2.53 to 3.44 ns.

The improvement of the fit with two correlation times over that with only one, as reflected in χ^2, is small but consistent for all of the four independent measurements.

Using Stokes–Einstein relationship [50] and a molecular weight of 8,400 Da for the Trp mutants, ϕ is equal to 3.0 ns. Taking the shape into account: an oblate ellipsoid of revolution with an axial ratio of 1:1.5 [4], would prolong $\phi \sim 1.2$ times [51], hence, ϕ is expected to be equal to 3.6 ns. This is still much shorter than the observed ~ 5.5 ns. Nevertheless this correlation time was measured two times with different labels. Covalent dimerization was ruled out by SDS-PAGE. Since nothing was reported about non-covalent dimerization from NMR experiments ($c \sim 7$ mM) [4], a phenomenon which should be strongly dependent on the concentration, it can be ruled out here ($c < 0.2$ mM), as well. Hence, the only explanation for the observed long correlation time is that the overall motion is slowed down by the C-terminal undecapeptide which is not put back to the body of the molecule but sticks out. Hence, Trp[2] and AEDANS-Cys[27] are attached to the core and rotate with the entire molecule, which is in accordance with the steady state and lifetime behaviour of both. The mobility of Trp[64] is increased (compared to Trp[2]) but not sufficiently to let two correlation times become apparent as in the case of Trp[70]. Nevertheless, the Trp[70] side chain still experiences steric hindrance. The mobility of Trp[70] is not as high as that of the Trp residue in the random coil peptide P10, where it makes that the overall motion of the peptide is not detectable any more.

3.5. Fluorescence energy transfer

To measure the distance $Trp^{70} \rightarrow$ AEDANS-Cys^{27} the so-called Förster distance had to be determined first. The overlap integral, J, was equal to 5.59×10^{-15} cm^3M^{-1} and the absolute quantum yield, Q_D, of Trp^{70} equal to 0.074. Together with $k^2 = 2/3$ this resulted in $R_0(2/3) =$ 20.3 Å which is in good agreement with previous results [35, 40]. Taking the high degree of labelling into account ($f_A = 0.85$, thus confirming that Cys^{27} is indeed pointing into the solution [4]) the transfer efficiencies resulting from steady-state and time-resolved measurements were 34% and 20% respectively, yielding $r_{(\text{steady state})} = 22.7$ Å and $r_{(\text{time-resolved})} = 25.6$ Å.

This difference, with $\langle \tau_{DA} \rangle / \langle \tau_D \rangle > F_{DA}/F_D$, is indicative of a distribution of chromophore separations [39]. The form of the distribution is usually not known but is reasonably represented by a Gaussian function. It is then possible to numerically evaluate the average separation $\langle r \rangle$ and the standard deviation σ. The results of this calculation can be gathered from Figs. 1 and 2 in ref. [39]. Based on $\langle \tau_{DA} \rangle / \langle \tau_D \rangle = 0.80$ and $F_{DA}/F_D = 0.66$ the average separation is 24.4 Å and the standard deviation 8.1 Å. The probability that the actual separation finds itself within 24.4 ± 8.1 Å is 68% and within 24.4 ± 16.2 Å is 95%.

There are two possible origins of these widths: They can either be due to the effect of k^2 on the transfer rates or to the mobility of donor and/or acceptor [40]. According to the formalism developed by Dale et al. [33] the maximum and minimum values of k^2 can be calculated from the orientation factors $d^X = (r_i/r_0')^{1/2}$, r_0' is the fundamental anisotropy measured in a vitrified solution and r_i is the amplitude of the anisotropy decay which is due to overall rotational diffusion of either donor or acceptor [40]. With r_i from Table 3 and r_0' from Table 6 in reference [40] one obtains: $d^D = \{(0.022 + 0.049)/0.238\}^{1/2} = (0.071/0.238)^{1/2} = 0.55$ and $d^A = (0.171/0.25)^{1/2} = 0.83$. From Fig. 9 in reference [33] $k^2_{min} = 0.2$ and $k^2_{max} = 2.6$ can be gathered. The actual distance is then related to the average separation $\langle r \rangle$ (where k^2 is assumed to be 2/3): $r = (1.5k^2)^{1/6}\langle r \rangle$ [32] resulting in $r_{min} = 20.0$ Å and $r_{max} = 30.6$ Å. But with the Trp → AEDANS pair, the excitation spectrum of the acceptor shows mixed polarization [19] and, hence, the k^2 range could be expected to be significantly narrower [34]. Using Table 3 of ref. [34] and r_0' values of 0.25 for Trp and AEDANS [40], one obtains a range of distances from 0.91 to 1.12 times of the average separation, resulting in: $r_{min} = 22.2$ Å and $r_{max} = 27.3$ Å. Hence, it appears that the effects of k^2 can cause an uncertainty in r of ±2.5 Å, whereas the remaining ±5.6 Å (8.1 Å minus 2.5 Å) have to be attributed to the side-chain mobility.

4. Summary and conclusion

According to our data, Trp^2 is fixed within the protein matrix and moves with the protein as a whole. This is in agreement with the NMR data: Leu^2 is not part of the N-terminal helix (4–12) but it shows a d_{NN} nuclear Overhauser effect (NOE) with Lys^5 and the resolved structure even includes Thr^1 [4]. This supports the idea that the N-terminus is attached and simply serves to stabilize the C5a conformation [6].

The C-terminus of C5a is of prime importance for biological activity but no definite structure could be determined for this part of the molecule by NMR spectroscopy. Beyond Ile^{65} short NOE distances between both $H_\alpha(i)$ and $NH(i+1)$ as well as $NH(i)$ and $NH(i+1)$ were observed in the NMR spectra [52]. Since for helices $NH(i)$–$NH(i+1)$ NOEs are intense and $H_\alpha(i)$–$NH(i+1)$ NOEs vanishingly small, and exclusively $H_\alpha(i)$–$NH(i+1)$ NOEs are observed in the case of an extended structure; this is compatible neither with a helical nor with an extended chain conformation. A dynamic structural averaging weighted toward helicity would allow both NOE distances to be detected [52].

Our results show that the side-chain mobility increases from Trp^{64} to Trp^{70}. But it does not reach that of a Trp in the random coil peptide P10 and the fluorescence energy transfer revealed an average distance of 24.4 ± 8.1 Å between Trp^{70} and AEDANS-Cys^{27}, though ±2.5 Å have to be attributed to the uncertainty in k^2.

This distribution of separations has its origin mainly in the mobility of Trp^{70} since AEDANS-Cys^{27} is fixed on the surface of the molecule.

The distance between C_α of Cys^{27} and C_α of Arg^{62} was calculated to be 13.5 Å based on the NMR structure of bovine C5a [3]. Supposed this distance is held constant by the core and either an α-helix or an extended peptide chain (distance between C_α of Ala^{63} and C_α of Met^{70} is 9.4 and 23 Å, respectively) is linked then the distance between Cys^{27} and Met^{70} varies from 22.9 Å in the case of a helix to 36.5 Å in the case of a fully extended chain. Hence, a slightly stretched helix fits much better the experimental results and it would also explain the restriction of the side-chain movement. Of course, this helix is not completely rigid as indicated by the width of the distance distribution.

To check whether this width is reasonable or not it can be compared with results obtained with rabbit troponin I [40]. The same donor–acceptor pair was used and nearly the same average distance and a similar width was determined for the distance distribution between Trp^{158} (Trp^{157} according to [53]) and Cys^{133}: FWHM = 11.5 Å; 11.5 Å/(2 × 1.18) = 4.9 Å = σ. Troponin I is approximately three times as big as C5a, and is expected to exist as a fairly open structure [53]. The FWHM is increased to 56 Å upon denaturation [40]. Hence, the C-terminus of C5a seems to possess an open structure but is far from being a random coil.

Since no long-range NOEs were observed between residues of the C-terminal peptide and other parts of the molecule, it seems that the C-terminal peptide does not preferentially dock to any region of the core of C5a [4] and, hence, points into solution. This would explain the long overall rotational correlation time because a hinged C-terminal rod would provide additional hydrodynamic resistance. Furthermore, the alternative compatible with the measured short distance between Cys^{27} and Met^{70}, a turn that folds back to the core is ruled out. Hence, the results of Zuiderweg et al. [4] and those presented here are consistent with the predominant existance of a flexible helix pointing into the solution.

The C-terminal peptide analogues are full agonists but far from being as potent as the natural C5a [8]. This is due to the absence of additional receptor binding sites [8] but a reduced tendency to adopt a high affinity conformation might also come into play.

Acknowledgements

Thanks are due to following members of the Institut für Biochemie: Manfred Dewor for the amino acid analyses, to Jürgen Stahl for the CD measurements, to Berthold Wroblowski for determining the secondary structural composition of rhC5a on the bases of these results and to Edgar Jacoby for computer graphic distance determinations. Furthermore, we wish to thank Dr. G. Marius Clore for providing the backbone coordinates of the NMR structure of bovine C5a. This work was supported by a grant from the Bundesminister für Forschung und Technologie der Bundesrepublik Deutschland (Förderkennzeichen 01 VM 8901/4).

References

1 D. Bitter-Suermann, in: The complement system, eds. K. Rother and G.O. Till (Springer Verlag, Berlin, 1988) 367.
2 W. Bautsch, M. Emde, T. Kretzschmar, J. Köhl, D. Suckau and D. Bitter-Suermann, Immunobiol. 185 (1992) 41.
3 J. Zarbock, R. Gennaro, D. Romeo, G.M. Clore and A.M. Gronenborn, FEBS Lett. 238 (1988) 289.
4 E.R.P. Zuiderweg, D.G. Nettesheim, K.W. Mollison and G.W. Carter, Biochemistry 28 (1989) 172.
5 M.P. Williamson and V.S. Madison, Biochemistry 29 (1990) 2895.
6 K.W. Mollison, W. Mandecki, E.R.P. Zuiderweg, L. Fayer, T.A. Fey, R.A. Krause, R.G. Conway, L. Miller, R.P. Edalji, M.A. Shallcross, B. Lane, J.L. Fox, J. Greer and G.W. Carter, Proc. Natl. Acad. Sci. USA 86 (1989) 292.
7 Y.S. Or, R.F. Clark, B. Lane, K.W. Mollison, G.W. Carter and J.R. Luly, J. Med. Chem. 35 (1992) 402.
8 J.A. Ember, S.D. Sanderson, S.M. Taylor, M. Kawahara and T.E. Hugli, J. Immunol. 148 (1992) 3165.
9 D.G. Nettesheim, R.P. Edalji, K.W. Mollison, J. Greer and E.R.P. Zuiderweg, Proc. Natl. Acad. Sci. USA 85 (1988) 5036.
10 R. Huber, H. Scholze, E.P. Pâques and J. Deisenhofer, Hoppe-Seyler Biol. Chem. 361 (1980) 1389.
11 J. Greer, Science 228 (1985) 1055.

12 C.J. Smith, A.R. Clarke, W.N. Chia, L.I. Irons, T. Atkinson and J.J. Holbrook, Biochemistry 30 (1991) 1028.
13 J.R. Lakowicz, I. Gryczynski, H. Szmacinski, H. Cherek and N. Joshi, Eur. Biophys. J. 19 (1991) 125.
14 W. Bautsch, T. Kretzschmar, T. Stühmer, A. Kola, M. Emde, J. Köhl, A. Klos and D. Bitter-Suermann, Biochem. J. 288 (1992) 261.
15 R. Higuchi, B. Krummel and R.K. Saiki, Nucleic Acids Res. 16 (1988), 7351.
16 D.H. Spackman, W.H. Stein and S. Moore, Anal. Chem. 30 (1958) 1190.
17 J.R. Benson and P.E. Hare, Proc. Natl. Acad. Sci. USA 72 (1975) 619.
18 N.P. Gerard, M.K. Hodges, J.M. Drazen, P.F. Weller and C. Gerard, J. Biol. Chem. 264 (1989) 1760.
19 E.N. Hudson and G. Weber, Biochemistry 12 (1973) 4154.
20 C.K. Wang and H.C. Cheung, J. Mol. Biol. 190 (1986) 509.
21 T.E. Creighton, in: Protein structure—A practical approach, ed. T.E. Creighton (IRL Press, Oxford, 1989) pp. 155–167.
22 H. Mach, C.R. Middaugh and R.V. Lewis, Anal. Biochem. 200 (1992) 74.
23 T.E. Hugli and H.J. Müller-Eberhard, Adv. Immunol. 26 (1978) 1.
24 G.C. Chen and J.T. Yang, Anal. Lett. 10 (1977) 1195.
25 H. Renscheidt, W. Straßburger, U. Glatter, A. Wollmer, G.G. Dodson and D.A. Mercola, Eur. J. Biochem. 142 (1984) 7.
26 S.W. Provencher and J. Glöckner, Biochemistry 20 (1981) 33.
27 J.P. Hennessey, Jr., and W.C. Johnson, Jr., Biochemistry 20 (1981) 1085.
28 H. Leismann, H.D. Scharf, W. Straßburger and A. Wollmer, J. Photochem. 21 (1983) 275.
29 I. Munro, I. Pecht and L. Stryer, Proc. Natl. Acad. Sci. USA 76 (1979) 56.
30 A.G. Szabo and D.M. Rayner, J. Am. Chem. Soc. 102 (1980) 554.
31 M. Federwisch, M. Casaretto, R. Gerardy-Schahn, D. Bitter-Suermann and A. Wollmer, Biophys. Chem. 44 (1992) 151.
32 L. Stryer, Annu. Rev. Biochem. 47 (1978) 819.
33 R.E. Dale, J. Eisinger and W.E. Blumberg, Biophys. J. 26 (1979) 161.
34 E. Haas, E. Katchalski-Katzir and I.Z. Steinberg, Biochemistry 17 (1978) 5064.
35 H.D. Schulzki, B. Kramer, J. Fleischhauer, D.A. Mercola and A. Wollmer, Eur. J. Biochem. 189 (1990) 683.
36 J.B. Birks, J. Res. Natl. Bur. Stand. (U.S.A.) 80A (1976) 389.
37 W.H. Melhuish, J. Phys. Chem. 65 (1961) 229.
38 S. Albaugh and R.F. Steiner, J. Phys. Chem. 93 (1989) 8013.
39 S. Albaugh, J. Lan and R.F. Steiner, Biophys. Chem. 33 (1989) 71.
40 J.R. Lakowicz, I. Gryczynski, H.C. Cheung, C.K. Wang, M.L. Johnson and N. Joshi, Biochemistry 27 (1988) 9149.
41 C. Gerard, D.E. Chenoweth and T.E. Hugli, J. Immunol. 127 (1981) 1978.
42 W.T. Morgan, E.H. Vallota and H.J. Müller-Eberhard, Biochem. Biophys. Res. Commun. 57 (1974) 572.
43 R. Gennaro, T. Simonic, A. Negri, C. Mottola, C. Secchi, S. Ronchi and D. Romeo, Eur. J. Biochem. 155 (1986) 77.
44 O. Shimizu, J. Watanabe and K. Imakubo, Photochem. Photobiol. 29 (1979) 915.
45 R.W. Cowgill, in: Biochemical fluorescence: Concepts, eds. R.F. Chen and H. Edelhoch (Marcel Dekker, New York, 1976) p. 441–486.
46 E.A. Burstein, N.S. Vedenkina and M.N. Ivkova, Photochem. Photobiol. 18 (1973) 263.
47 J.M. Beechem and L. Brand, Annu. Rev. Biochem. 54 (1985) 43.
48 R. Rigler, J. Roslund and S. Forsen, Eur. J. Biochem. 188 (1990) 541.
49 J.R. Lakowicz, H. Cherek, I. Gryczynski, N. Joshi and M.L. Johnson, Biophys. J. 51 (1987) 755.
50 E. Bucci and R.F. Steiner, Biophys. Chem. 30 (1988) 199.
51 E.W. Small and I. Isenberg, Biopolymers 16 (1977) 1907.
52 E.R.P. Zuiderweg, J. Henkin, K.W. Mollison, G.W. Carter and J. Greer, Proteins Struct. Func. Genet. 3 (1988) 139.
53 J.M. Wilkinson and R.J.A. Grand, Nature 271 (1978) 31.